Neuron, Vol. 34, 877–884, June 13, 2002, Copyright ©2002 by Cell Press

Molecular Basis of an Inherited Epilepsy

Christoph Lossin,[1,2] Dao W. Wang,[1,4] Thomas H. Rhodes,[1] Carlos G. Vanoye,[1,3] and Alfred L. George, Jr.[1,2,3,4,5]
[1]Division of Genetic Medicine
[2]Center for Molecular Neurosciences
[3]Department of Medicine
[4]Department of Pharmacology
Vanderbilt University
Nashville, Tennessee 37232

Summary

Epilepsy is a common neurological condition that reflects neuronal hyperexcitability arising from largely unknown cellular and molecular mechanisms. In generalized epilepsy with febrile seizures plus, an autosomal dominant epilepsy syndrome, mutations in three genes coding for voltage-gated sodium channel α or β1 subunits (*SCN1A*, *SCN2A*, *SCN1B*) and one GABA receptor subunit gene (*GABRG2*) have been identified. Here, we characterize the functional effects of three mutations in the human neuronal sodium channel α subunit SCN1A by heterologous expression with its known accessory subunits, β1 and β2, in cultured mammalian cells. SCN1A mutations alter channel inactivation, resulting in persistent inward sodium current. This gain-of-function abnormality will likely enhance excitability of neuronal membranes by causing prolonged membrane depolarization, a plausible underlying biophysical mechanism responsible for this inherited human epilepsy.

Introduction

Idiopathic epilepsy is a common, paroxysmal, and clinically heterogeneous neurological disorder with incompletely understood cellular mechanisms (Browne and Holmes, 2001; McCormick and Contreras, 2001; Shin and McNamara, 1994). While many factors contribute to the pathogenesis of epilepsy, a subset of familial epilepsy syndromes are "channelopathies," inherited conditions caused by mutations in genes encoding various voltage-gated and ligand-gated ion channels (Berkovic, 2001; Meisler et al., 2001). Among these disorders are genetically distinct forms of generalized epilepsy with febrile seizures plus (GEFS+), an autosomal dominant syndrome characterized by febrile seizures and various types of afebrile seizures (Scheffer and Berkovic, 1997; Singh et al., 1999). GEFS+ has previously been linked to mutations in genes encoding voltage-gated sodium channel α (*SCN1A*, *SCN2A*) (Escayg et al., 2000; Sugawara et al., 2001a) or β1 (*SCN1B*) (Wallace et al., 1998) subunits and one GABA receptor subunit (*GABRG2*) (Baulac et al., 2001; Wallace et al., 2001a). Mutations in *SCN1A* represent the most frequent cause of the disease (Abou-Khalil et al., 2001; Escayg et al., 2001; Sugawara et al., 2001b; Wallace et al., 2001b). A closely related inherited epilepsy, severe myoclonic epilepsy of infancy, has also been associated with *SCN1A* mutations (Claes et al., 2001).

Throughout the central nervous system, voltage-gated sodium channels are critical for the generation and propagation of action potentials and serve as important pharmacological targets for anticonvulsant agents (Catterall, 1999; Macdonald and Greenfield, 1997). The pathological role of sodium channel mutations in epilepsy is not well understood. Therefore, functional characterization of disease-associated mutant sodium channel alleles may shed new light on the molecular basis of GEFS+ specifically, advance our understanding of epileptogenesis in general, and provide information useful for the design of new therapeutic interventions. Although two groups have previously investigated the functional consequences of GEFS+ *SCN1A* mutations using recombinant sodium channels (Alekov et al., 2000, 2001; Spampanato et al., 2001), no studies have examined mutations in the authentic human SCN1A channel in the presence of β1 and β2 subunits.

We report here the successful cloning and functional characterization of human SCN1A along with electrophysiological experiments demonstrating biophysical disturbances conferred by three distinct GEFS+ mutations. Our findings indicate that GEFS+ is caused by a defect in sodium channel inactivation that leads to a persistent inward current during sustained depolarizations. This defect will likely cause prolonged neuronal depolarization leading to increased firing frequency and enhanced excitability.

Results

Cloning and Functional Expression of Human SCN1A

The complete coding region (6030 bp) of human SCN1A (designated $Na_v1.1$ by some authors) (Goldin et al., 2000) with 873 bp of the 3′ untranslated region was deduced from a publicly available genomic sequence and isolated as four overlapping cDNAs using reverse-transcriptase polymerase chain reaction (RT-PCR) cloning as defined in Experimental Procedures. The predicted 2009 amino acid peptide exactly matches the sequence reported by Escayg et al. (2000) (GenBank accession number P35498). Two probable splice variants were also identified through sequencing of independently isolated cDNAs. Both variants result from utilization of alternative splice donor sequences contained within exon 11 and produce in-frame deletions of 33 and 84 nucleotides (encoding a portion of the cytoplasmic region between domains I and II). The assembled SCN1A cDNA (nonvariant form) in a mammalian expression plasmid was transiently transfected into tsA201 cells along with plasmids encoding the human β1 and β2 sodium channel subunits coupled to distinct reporter genes (CD8 antigen and green fluorescent protein, respectively). Transfected cells expressing both reporters and exhibiting voltage-

[5]Correspondence: al.george@vanderbilt.edu

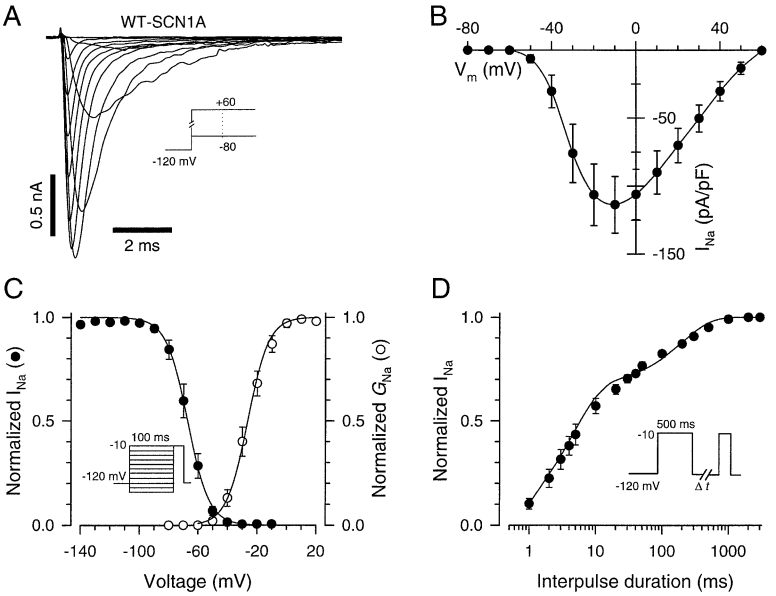

Figure 1. Functional Characterization of WT-SCN1A in tsA201 Cells

(A) Typical current tracings from a tsA201 cell transiently transfected with WT-SCN1A, hβ1, and hβ2 recorded at various test potentials between −80 and +50 mV (holding potential was −120 mV).

(B) Current-voltage relationship for WT-SCN1A. Whole-cell currents were normalized to cell capacitance (n = 8).

(C) Voltage dependence of sodium channel availability and activation. The voltage dependence of sodium channel availability (steady-state inactivation) was obtained using a standard double-pulse protocol indicated as an inset. Half-maximal inactivation was reached at −67.5 ± 2.3 mV with a slope factor of −6.2 ± 0.3 (n = 9). Half-maximal activation occurred at −26.4 ± 2.3 mV with a slope factor of 7.1 ± 0.2 (n = 8).

(D) Time course of recovery from inactivation at −120 mV. The pulse protocol for measuring recovery from inactivation is shown as an inset. The time constants and fractional amplitudes (given in parentheses) were as follows: τ_f = 6.4 ± 1.3 ms (71% ± 3%), τ_s = 263 ± 36 ms (29% ± 3%), n = 9.

dependent inward sodium current were used for electrophysiological experiments.

Figure 1 illustrates the biophysical behavior of recombinant human wild-type SCN1A (WT-SCN1A) coexpressed with human β1 and β2 subunits. Rapidly activating and inactivating voltage-dependent inward currents were observed in response to depolarizing test potentials and were generally robust (typical peak current amplitude range 1–5 nA; Figure 1A). Endogenous inward currents larger than 0.2 nA were never observed in nontransfected cells. Peak activation of sodium current occurred at −10 mV (Figure 1B), and the expressed currents were highly tetrodotoxin (TTX) sensitive (data not shown). Voltage-dependent channel availability and activation were half-maximal at −67.5 ± 2.3 and −26.4 ± 2.3 mV, respectively (Figure 1C). Recovery from inactivation following a 500 ms depolarization exhibited two exponential components (Figure 1D), with a predominant fast (time constant, τ_f = 6.4 ± 1.3 ms, 71% ± 3%) and smaller slow component (τ_s = 263 ± 36 ms, 29% ± 3%). All of these properties are consistent with voltage-gated sodium channels and closely resemble previously described native human neuronal sodium channel activities (Reckziegel et al., 1998; Sah, 1995).

Epilepsy-Associated SCN1A Mutants Alter Inactivation

We examined the biophysical properties of three GEFS+ mutants using recombinant human SCN1A sodium channels. Figures 2A–2C illustrate typical whole-cell recordings obtained from cells expressing T875M, W1204R, or R1648H. All three mutants exhibited robust, rapidly activating and inactivating inward currents in response to a series of test depolarizations. However, close examination of all recordings revealed the presence of noninactivating inward current in the mutants that was not observed in WT-SCN1A. This noninactivating current was evident during a longer test depolarization (100 ms) and could be reversibly and completely blocked by the application of 10 μM TTX, thus excluding a leak current (Figure 2D). The size of the noninactivating current varied among the mutants, but was largest in R1648H-expressing cells (in percent of peak current: WT-SCN1A, 0.2% ± 0.1%, n = 4; R1648H, 4.2% ± 0.6%, n = 5, $p < 0.0005$ versus WT-SCN1A; T875M, 1.5% ± 0.2%, n = 4, $p < 0.001$ versus WT-SCN1A; W1204R, 0.9% ± 0.2%, n = 8, $p < 0.01$ versus WT-SCN1A). A characteristic displayed by noninactivating sodium channels is the inappropriate activation of inward current during a slow depolarization. This feature was demonstrated by comparing the responses of WT-SCN1A to R1648H using the voltage-ramp protocol illustrated in Figure 3. Slow membrane depolarization triggered a significantly larger inward current in cells expressing R1648H than in WT-SCN1A-expressing cells (maximal ramp current divided by the peak transient current × 100 [mean ± SEM]: WT-SCN1A, 0.3 ± 0.08%; n = 6 versus R1648H, 1.9 ± 0.2%; n = 5, $p < 0.0001$).

This inactivation disturbance was previously not observed when similar GEFS+ mutations were examined in the human skeletal muscle sodium channel (Alekov et al., 2000, 2001) or the rat SCN1A ortholog (Spampanato et al., 2001), suggesting that species and isoform-related variables may be important for revealing this mutant sodium channel phenotype. Furthermore, the absence of persistent sodium currents in the work reported by Spampanato et al. (2001) may relate to abnormal inactivation properties commonly observed for recombinant neuronal and muscle sodium channels expressed in *Xenopus* oocytes (Krafte et al., 1990; Moorman et al., 1990; Zhou et al., 1991).

Mutant sodium channels expressed similar current density as WT-SCN1A (Figure 4A) and exhibited no significant differences in the voltage dependence of inactivation time constants (Figure 4B). Other biophysical properties of the mutant sodium channels grossly resembled those of WT-SCN1A, with three exceptions. A significant depolarizing shift in the voltage dependence

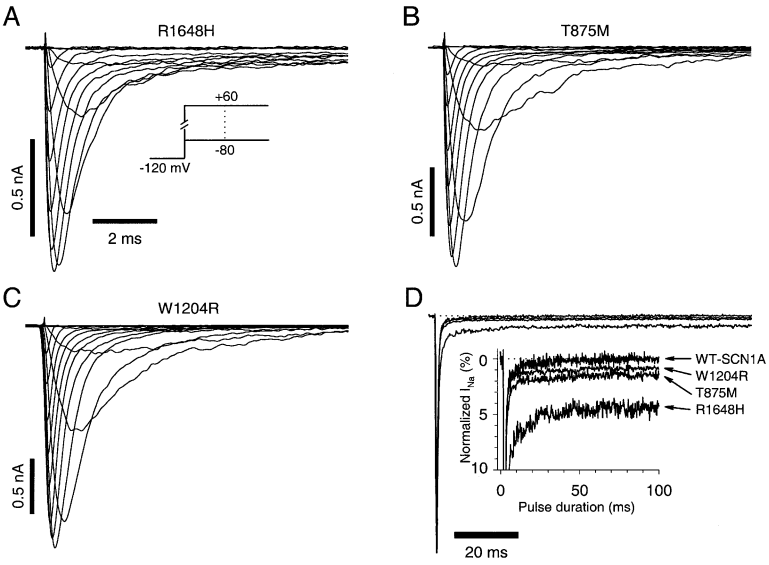

Figure 2. Whole-Cell Recordings of Mutant SCN1A Channels

Typical current tracings from transiently transfected tsA201 cells expressing SCN1A mutants R1648H (A), T875M (B), and W1204R (C) recorded at various test potentials between −80 and +50 mV stepped from a holding potential of −120 mV. In all experiments, hβ1 and hβ2 were coexpressed. (D) Representative WT-SCN1A, R1648H, T875M, and W1204R TTX-sensitive sodium currents. Sodium current was elicited by a 100 ms depolarization from −120 to −10 mV. TTX-sensitive currents were obtained by digital subtraction of sodium currents recorded before and after TTX addition. Peak sodium currents were normalized. Zero-current level is indicated by a dotted line. The inset shows an expanded *y* axis scaled to emphasize the relative proportion of noninactivating current.

of channel availability was exhibited by T875M, and a significant hyperpolarizing shift of channel activation was observed for W1204R (Figure 4C). There was also an enhancement of the slow component of recovery from inactivation observed for T875M and R1648H (Figure 4D). The most consistent defect observed for all three mutant sodium channels was the presence of a noninactivating current component.

Single-Channel Analysis

We recorded sodium currents in excised outside-out patches from cells expressing either WT-SCN1A or the R1648H mutant to resolve single-channel behavior. Figures 5A and 5B illustrate representative patch clamp recordings from the two conditions. Wild-type sodium channels exhibited predominantly early, short-lived (< 1 ms) openings followed by infrequent late openings and rare short bursts of reopenings. By contrast, mutant sodium channels exhibited a much higher probability of late openings occurring throughout 200 ms test depolarizations. Multiple late openings were seen in all sweeps recorded from mutant sodium channel patches. Estimated single-channel conductance at the examined test potential was not different between alleles (WT-SCN1A, 16.6 ± 0.7 pS [n = 7] versus R1648H, 17.3 ± 0.5 pS [n = 5]; test potential was 0 mV). Ensemble average currents generated from ~400 individual sweeps (Figure 5C) closely resembled the whole-cell data presented in Figures 1 and 2. These data indicate a significant inactivation defect present in R1648H channels that explains the disturbance in sodium channel behavior observed in whole-cell recordings (Figure 2D).

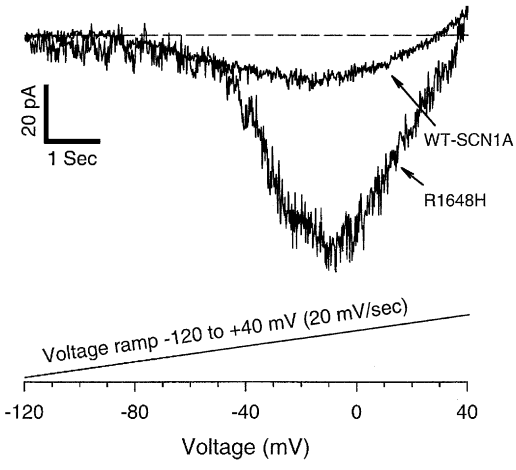

Figure 3. Responses of WT-SCN1A and R1648H to Ramp Depolarization

Cells were initially voltage clamped to a holding potential of −120 mV to assure all sodium channels were available. The membrane potential was slowly ramped from −120 mV to +40 mV over 8 s (20 mV/s). Traces represent TTX-sensitive currents obtained by digital subtraction of sodium currents recorded before and after TTX (10 μM) addition. The dashed line indicates the zero current level. A representative experiment is illustrated (the peak transient sodium currents were −3.6 nA for WT-SCN1A and −3.2 nA for R1648H). Similar experimental results were observed in four cells for WT-SCN1A and five cells for R1648H.

Discussion

We have extensively investigated the biophysical properties of three distinct GEFS+ mutations using recombinant human SCN1A coexpressed heterologously in cultured mammalian cells with human accessory subunits β1 and β2. Because all essential molecular elements necessary for assembly of human neuronal sodium channels (Catterall, 1992) were provided, our experiments have a high likelihood of revealing the true functional defect responsible for this disease. Using this approach, we also circumvented potential concerns regarding the molecular context of previous characterizations of GEFS+ mutations in nonhuman or nonneuronal sodium channels expressed in the absence of one or both β subunits (Alekov et al., 2000, 2001; Spampanato et al., 2001). Such variability in experimental conditions may explain critical differences between our observations and those of other investigators.

Our data demonstrate a clear defect in channel inactivation exhibited by the GEFS+ mutations T875M,

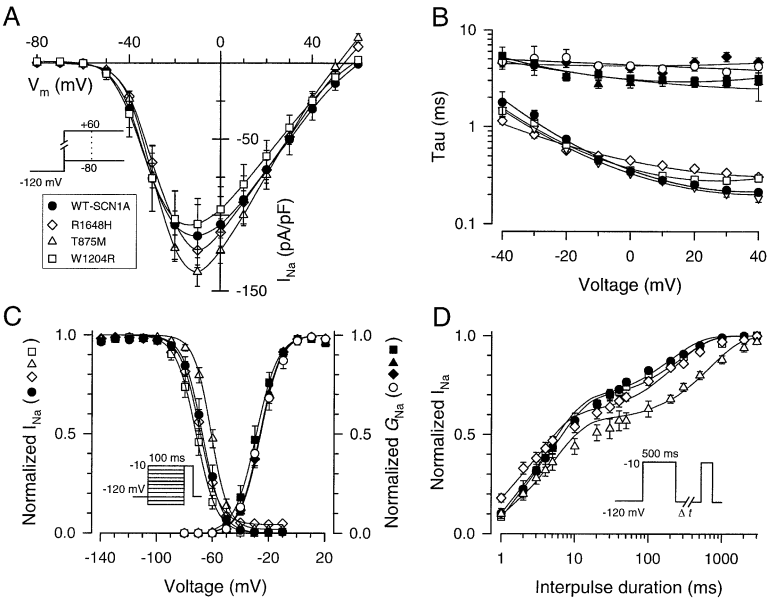

Figure 4. Biophysical Characterization of Mutant SCN1A Channels

(A) Current-voltage relationships of WT-SCN1A, R1648H, T875M, and W1204R. Whole-cell currents were normalized to cell capacitance and plotted against the test potential (n = 8–19).

(B) Voltage dependence of fast inactivation time constants for wild-type and mutant channels. Symbol shapes are defined in the inset of (A). Data representing fast and slow time constants of mutant channels are shown as open and closed symbols, respectively. Symbols representing wild-type data appear with the opposite shading pattern.

(C) Voltage dependence of sodium channel availability and activation (symbol definitions are similar to those in the inset of [A], and the shading pattern is given in the *y* axis legends). The pulse protocol shown as an inset refers to channel availability only. The membrane potentials for half-maximal inactivation and slope factors were as follows (values for WT-SCN1A are given in the Figure 1 legend): R1648H, −69.1 ± 2.1 mV and −6.5 ± 0.4, n = 10; T875M, −60.7 ± 1.1 mV ($p < 0.01$ versus WT-SCN1A) and −5.9 ± 0.6, n = 13; W1204R, −72.0 ± 2.0 mV and −6.9 ± 0.4, n = 7. The activation curve was constructed as described in the legend of Figure 1. Half-maximal activation occurred at the following potentials: R1648H, −25.9 ± 1 mV (n = 15); T875M, −26.1 ± 1.2 mV (n = 19); W1204R, −29.6 ± 1.2 mV (n = 9, $p < 0.005$ versus WT-SCN1A). Slope factors of the mutants were not significantly different from that of WT-SCN1A (data not shown).

(D) Recovery from inactivation. Data were acquired according to the pulse protocol shown as an inset (symbol definitions given in the inset of [A]). The time constants and fractional amplitudes (given in parentheses) were as follows (values for WT-SCN1A are given in Figure 1 legend): R1648H, τ_f = 3.1 ± 0.2 ms (60% ± 4%), τ_s = 257 ± 36 ms (40% ± 4%), n = 9 ($p < 0.05$ for τ_s and fractional amplitudes); T875M, τ_f = 4.6 ± 0.5 ms (55% ± 5%), τ_s = 680 ± 151 ms (45% ± 5%), n = 10 ($p < 0.05$ for τ_s and fractional amplitudes); W1204R, τ_f = 5.3 ± 0.5 ms (68% ± 2%), τ_s = 244 ± 31 ms (32% ± 2%), n = 8.

W1204R, and R1648H. The observation of a significant persistent noninactivating current component in all three mutants studied suggests that gain-of-function (i.e., increased sodium conductance) may be responsible for seizure susceptibility in this syndrome. This behavior is reminiscent of the channel dysfunction associated with two other human sodium channelopathies: hyperkalemic periodic paralysis and congenital long QT syndrome. Mutations in genes encoding the muscle sodium channel (*SCN4A*) (Cannon, 2000) or the cardiac sodium channel (*SCN5A*) (Bennett et al., 1995) have been demonstrated to cause defects in fast inactivation manifesting as a small but significant noninactivating late sodium current. Interestingly, at the tissue level, this type of channel dysfunction may result in increased excitability, giving rise to myotonia in skeletal muscle and ventricular arrhythmia in the heart. In muscle, however, persistent depolarization of the sarcolemma can also cause widespread inactivation of normal sodium channels, leading to excitation failure and paralysis (Cannon et al., 1993).

Our data provide an important insight into the pathophysiology of sodium channel dysfunction in epilepsy. We speculate that a small noninactivating inward current facilitates neuronal hyperexcitability because of a reduced threshold for action potential firing. The noninactivating currents we observed in cells expressing GEFS+ mutants may correlate with characteristic interictal activity, known as paroxysmal depolarization shifts, observed in epileptic foci and in vitro models of epileptic neuronal circuits (Ayala et al., 1970; Matsumoto and Ajmone-Marsan, 1964; Segal, 1991, 1994). Altered sodium channel function could also lead to a number of other secondary cellular consequences, such as increased potassium efflux during repolarization, that may also contribute to neuronal hyperexcitability (Dudek et al., 1998; Jefferys, 1995). Determining the precise cellular consequences of this defect in the nervous system requires further study.

The variable magnitude of noninactivating current that we observed for the three distinct GEFS+ mutations may potentially correlate with the severity of the phenotype, although genotype-phenotype relationships are difficult to construct reliably at this point from the small number of reported families. Other biophysical disturbances were also observed in the SCN1A mutants, but none were exhibited uniformly by all alleles. For mutants T875M and W1204R, differences in the voltage dependence of inactivation and activation, respectively, are consistent with a gain-of-function. However, the enhancements in the slow component of recovery from inactivation observed for T875M and R1648H may result in reduced sodium current density during long depolarizations or repetitive stimulation. These additional functional defects may help explain subtle phenotypic differences between individuals carrying different mutations, but more work is needed to make these associations.

Genetic modifiers and environmental factors are also likely to impact substantially on disease expression. Individuals with GEFS+ appear to have an intrinsic seizure-prone condition in which seizures may be triggered by fever or other unidentified nonfebrile factors (Scheffer

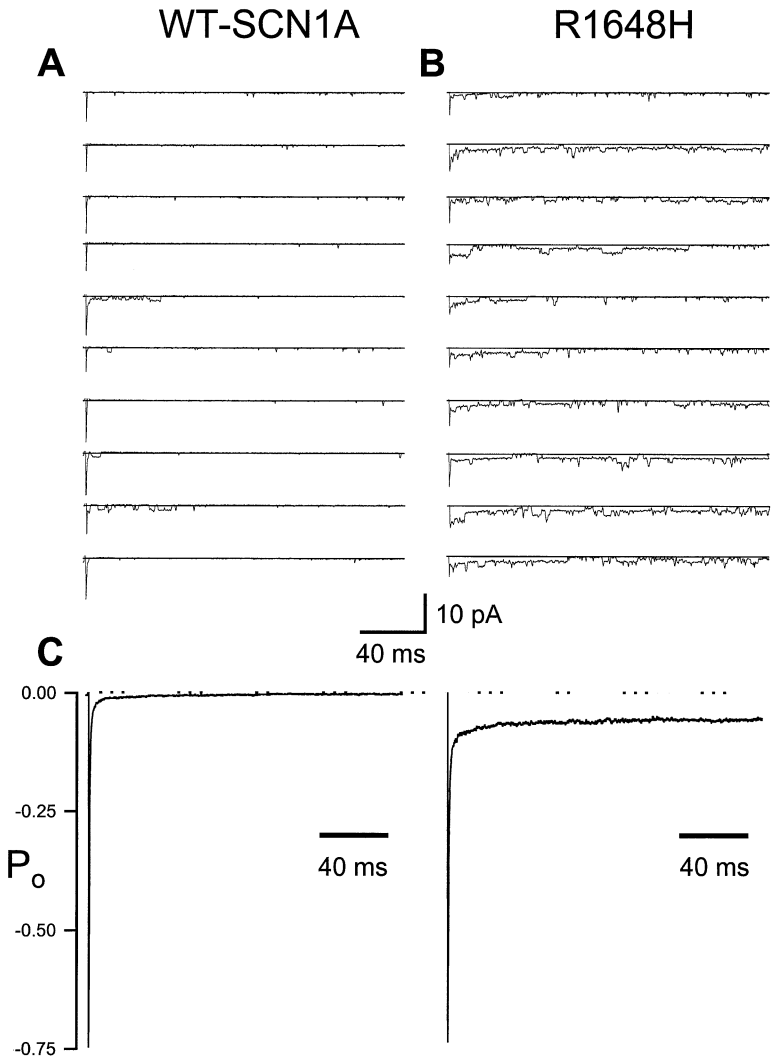

Figure 5. Single-Channel Recordings of WT-SCN1A and R1648H

Representative single-channel traces recorded in outside-out membrane patches excised from tsA201 cells transiently transfected with WT-SCN1A (A) or R1648H (B) plus hβ1 and hβ2 subunits. The number of channels per patch was estimated to be ~18 channels for WT-SCN1A and ~11 channels for R1648H by dividing the largest current peak measured during 100 sweeps by the unitary conductance. Channel openings are shown as downward deflections and solid horizontal lines indicate zero-current level. Channel activity was measured for 200 ms at 0 mV from a holding potential of −100 mV. (C) Ensemble average currents for WT-SCN1A and R1648H generated from single-channel data. Four independent experiments for each channel allele (100 sweeps per experiment) were averaged. The vertical axis depicts open probability (P_o) obtained by dividing the ensemble average current by the unitary current (~1 pA) and the number of channels per patch.

and Berkovic, 1997; Singh et al., 1999). Fever appears to be an important nongenetic factor in the triggering of seizures in GEFS+. At this time, we chose not to specifically examine differences in temperature sensitivity between wild-type and mutant SCN1A alleles because of a variety of technical issues (increased thermal noise, excessively rapid gating kinetics, channel rundown) that make recordings of voltage-gated sodium channels at physiological temperatures unreliable. Also, seizure susceptibility in GEFS+ is not strictly linked to fever, and most forms of febrile seizures occur in the absence of known sodium channel defects.

As with many other epilepsy syndromes, GEFS+ patients exhibit multiple types of seizures, including partial and generalized forms (Abou-Khalil et al., 2001; Scheffer and Berkovic, 1997; Singh et al., 1999; Sugawara et al., 2001b). Such pleomorphism is difficult to explain solely on the basis of the sodium channel inactivation defect observed in our studies. We speculate that the underlying sodium channel dysfunction predisposes GEFS+ patients to seizures at an early age. Neuronal injury resulting secondarily to convulsions may then evoke pathological structural changes and chronically reduce seizure threshold (McCormick and Contreras, 2001). Epileptogenesis in GEFS+ may therefore be preventable by early pharmacological intervention that specifically targets the underlying sodium channel dysfunction. As persistent neuronal sodium currents may be a common underlying mechanism in some forms of epilepsy (Segal, 2002), further studies of the pharmacology of mutant SCN1A channels may provide an in vitro model system for testing and development of new anticonvulsants that specifically target this abnormal activity.

Experimental Procedures

Molecular Cloning of Human SCN1A cDNA

The human SCN1A open reading frame (ORF) was predicted by comparing the orthologous rat coding sequence (GenBank accession number NM_030875) to the human genomic sequence using the program BLASTN (http://www.ncbi.nlm.nih.gov/blast). Twenty-six exons were identified, ordered, and assembled into a 6030 bp ORF and 873 bp 3′ untranslated region (3′UTR). Based on this prediction, four sets of PCR primers (AF: 5′-GTTTCTTGCGGCCGCATG GAGCAAACAGTGCTTGTACCA-3′, AR: 5′-GTGT CTTTCCCTTCAAT GGAGAAGCGA-3′, BF: 5′-GTTTCTTCTGGTGGGGAAGAGA AAG-3′, BR: 5′-GTGTCTTCTATACCACTTGTAGTTCCATTTA-3′, CF: 5′-GTTT CTTTATGTCCAATCATACAGCAGA-3′, CR: 5′-GTGTCTTGGCTTAC

TGTTGAGAATGGG-3′, DF: 5′-GTTTCTTACGCCATTATTATTTTA CCA-3′, DR: 5′-GTGTCTTGTCGACTCAAGGTCATCTCCCCTTTA-3′) were designed to generate overlapping SCN1A cDNAs. Human cerebral cortex cDNA (Clontech, Palo Alto, CA) was used as template during hot-start PCR performed in 50 μl reactions at 94°C for 5 min followed by 35 cycles of 94°C for 1 min, 51°C–57°C for 1 min, and 72°C for 3–4 min, and a final cycle at 72°C for 5 min. Some reactions required the addition of 10% (v/v) Q solution (Qiagen, Valencia, CA). To enhance amplification fidelity, all reactions were performed using a combination of *Taq* and *Pwo*I (20% v/v; Roche, Indianapolis, IN) polymerases.

Reaction products were gel-extracted, then cloned into pCR2.1-TOPO (Invitrogen, Carlsbad, CA), and selectively grown in TOP10, INVαF′ (Invitrogen), or STBL2 cells (Life Technologies, Grand Island, NY). Plasmid DNA was isolated with standard techniques, confirmed by restriction fingerprinting, and sequenced using automated fluorescent dye terminator chemistry. Polymerase errors were repaired by site-directed mutagenesis or by subcloning fragments from other clones. A full-length cDNA was assembled in the mammalian expression vector pCMV-Script (Stratagene, La Jolla, CA) and resequenced completely. A short poly-T region exhibiting a high spontaneous mutation rate in the full-length construct was interrupted by the introduction of two silent T to C mutations at ORF positions 1206 and 1209. All full-length constructs were propagated in STBL2 cells grown at 30°C for >48 hr.

Mutagenesis

SCN1A mutants T875M, W1204R, and R1648H were named according to the single-letter code indicating the amino acid exchange and its position with respect to the starting methionine. Mutants were generated by PCR-based site-directed mutagenesis. Successful introduction of the mutations was monitored by digestion at engineered silent restriction sites, and all mutant cDNAs (complete coding regions) were resequenced fully before use in experiments.

Cell Culture and Transfection

Human tsA201 cells, a HEK-293 derivative stably transfected with the SV40 large T antigen, were grown in Dulbecco's modified Eagle's medium (DMEM) supplemented with 10% (v/v) fetal bovine serum (Atlanta Biologicals, Norcross, GA), 2 mM L-glutamine, and penicillin-streptomycin (50 units/ml and 50 μg/ml, respectively) in a humidified 5% CO_2 atmosphere at 37°C. Only cells from passages ≤ 13 were used.

Expression of SCN1A, β1, and β2 was achieved by transient plasmid transfection using Qiagen Superfect reagent. Approximately 6 μg of total DNA was transfected (plasmid mass ratio was α:β1:β2 = 10:1:1). The human voltage-gated sodium channel auxiliary subunits hβ1 and hβ2 were cloned into plasmids containing the marker genes CD8 (pCD8-IRES-hβ1) or GFP (pGFP-IRES-hβ2) along with an internal ribosome entry site. Cells were passaged 24 hr after transfection and incubated 24 hr before their use in electrophysiology experiments. Transfected cells were dissociated by brief exposure to trypsin/EDTA, resuspended in supplemented DMEM medium, and allowed to recover for ~30 min at 37°C in 5% CO_2. CD8 antibody-covered microbeads (Dynabeads M-450 CD8, Dynal, Norway) suspended in 200 μl DMEM were added to the cell suspension and gently shaken. In order to allow for patch excision in single-channel studies, tsA201 cells were plated on glass coverslips pretreated with CELL-TAK cell and tissue adhesive (Collaborative Biomedical Products, Bedford, MA). Only cells positive for CD8 antigen and GFP fluorescence were used for electrophysiological studies. Non-transfected cells were used as negative controls.

Electrophysiology and Data Analysis

Dissociated cells were placed into a recording chamber on the stage of an inverted microscope with epifluorescence capability. After allowing the cells to settle for 10 min, sodium currents were recorded in the whole-cell or excised, outside-out patch configuration of the patch-clamp technique (Hamill et al., 1981) using Axopatch 200 series amplifiers (Axon Instruments, Union City, CA). Bath solution (145 mM NaCl, 4 mM KCl, 1.8 mM $CaCl_2$, 1 mM $MgCl_2$, 10 mM HEPES [pH 7.35, 310 mOsm/kg]) was continuously exchanged by a gravity-driven perfusion system. The pipette solution (10 mM NaF, 110 mM CsF, 20 mM CsCl, 2 mM EGTA, 10 mM HEPES [pH 7.35, 310 mOsm/kg]) was matched in pH and osmolality to the bath solution. Patch pipettes were pulled from borosilicate glass (Warner Instrument, Hamden, CT) with a multistage P-97 Flaming-Brown micropipette puller (Sutter Instruments, San Rafael, CA) and fire-polished with a Micro Forge MF 830 (Narashige, Japan). Patch pipettes for single-channel studies were coated with Sylgard 184 (Dow Corning, Midland, MI). Pipette resistance was 0.8–1.5 MΩ for whole-cell and ~4 MΩ for single-channel experiments. Cells were allowed to stabilize for 10 min after establishment of the whole-cell configuration before currents were measured. Recordings from cells exhibiting peak current amplitudes less than 0.8 nA were excluded from analysis to avoid potential endogenous channel contamination. Cells exhibiting very large whole-cell currents were also excluded if voltage control was compromised. Whole-cell capacitance was assessed by integrating the capacitive transient elicited by a 10 mV voltage step from −120 mV to −110 mV with 10 kHz filtering. As a reference electrode, a 2% agar bridge with composition similar to the bath solution was utilized. Whole-cell currents were acquired at 20–50 kHz and filtered at 5 kHz. Single-channel current traces were acquired at 10 kHz and filtered at 1 kHz.

Channel behavior was examined over a range of test potentials (see figure insets for pulse protocols). Each voltage step was followed by a 5 s recovery period at −120 mV. Pulse generation, data collection, and analyses were done with pCLAMP 7.0 or 8.1 (Axon Instruments), Excel 97 (Microsoft, Seattle, WA), Origin 6.0 (Microcal, Northampton, MA), and Sigma Plot 2000 (SPSS Science, Chicago, IL) software. Current-voltage relationships were constructed by plotting the peak current against the test potential. Steady-state inactivation was analyzed by a two-pulse protocol, where the peak current measured during the test pulse was normalized to the prepulse peak current and plotted as open probability versus prepulse potential. Data were fitted to a two-state Boltzmann equation:

$$f(x) = \frac{1 - C}{e^{(x - V_{1/2})/k}} + C,$$

where $V_{1/2}$ is the voltage at which 50% of the channels are inactivated, k is the slope factor, and C is the steady-state asymptote. Time constants (τ) of inactivation were derived from the current decay fitted to a single or a double exponential function:

$$f(t) = \sum_{i=1}^{n} A_i \cdot e^{-(t - K)/\tau_i} + C,$$

where t is the time, A is the fraction of channels inactivating with time constant τ_i (τ_f and τ_s represent fast and slow time constants, respectively), and K is the manually selected point of onset of exponential macroscopic current decay. Data for determining the voltage dependence of activation was derived from calculating conductances using the formula:

$$G(V) = \frac{I(V)}{V - E_{rev}},$$

where $I(V)$ is the peak raw current at the clamping potential V, and E_{rev} is the estimated reversal potential. Conductances were normalized to the maximal conductance between −80 and +20 mV and fitted to the two-state Boltzmann equation:

$$f(x) = \frac{-1}{e^{(x - V_{1/2})/k}} + 1,$$

where $V_{1/2}$ is the voltage at which half-maximal activation occurs, and k describes the slope of the fit. Recovery from inactivation was also examined by a two-pulse protocol. The peak current amplitude during the test pulse was plotted as fractional recovery against the recovery period by normalizing to the maximum current during the conditioning, followed by fitting to a single or a double exponential function:

$$f(t) = \sum_{i=1}^{n} A_i (1 - e^{-t/\tau_i}),$$

where t is time, and A_i describes the fraction of channels recovering with τ_i (τ_f and τ_s represent fast and slow time constants, respectively).

All experiments were performed at room temperature. Data are

shown as means ± SEM with the number of experiments provided as n in the figure legends. Statistical comparisons were done with the Student's t test and differences were considered significant at the $p < 0.05$ level.

Acknowledgments

We thank Dr. Naomasa Makita for the generous gift of the pCD8-IRES-hβ1 plasmid and Megan Olarte for DNA sequencing. We also are grateful to Dr. Robert MacDonald for critical reading of the manuscript. This project was supported by NIH grant NS3287 (A.L.G.) and by a predoctoral fellowship award from the Epilepsy Foundation (C.L.). This project was also funded by the Epilepsy Foundation through the generosity of the Kathy Holden Genetic Research Fund and supported by a grant from the Roland and Ruby Holden Foundation on behalf of Ronald and Arlene Holden.

Received: January 14, 2002
Revised: April 12, 2002

References

Abou-Khalil, B., Ge, Q., Desai, R., Ryther, R., Bazyk, A., Bailey, R., Haines, J.L., Sutcliffe, J.S., and George, A.L., Jr. (2001). Partial epilepsy and generalized epilepsy with febrile seizures plus and a novel *SCN1A* mutation. Neurology *57*, 2265–2272.

Alekov, A., Rahman, M.M., Mitrovic, N., Lehmann-Horn, F., and Lerche, H. (2000). A sodium channel mutation causing epilepsy in man exhibits subtle defects in fast inactivation and activation in vitro. J. Physiol. (London) *529 Pt 3*, 533–539.

Alekov, A.K., Rahman, M.M., Mitrovic, N., Lehmann-Horn, F., and Lerche, H. (2001). Enhanced inactivation and acceleration of activation of the sodium channel associated with epilepsy in man. Eur. J. Neurosci. *13*, 2171–2176.

Ayala, G.F., Matsumoto, H., and Gumnit, R.J. (1970). Excitability changes and inhibitory mechanisms in neocortical neurons during seizures. J. Neurophysiol. *33*, 73–85.

Baulac, S., Huberfeld, G., Gourfinkel-An, I., Mitropoulou, G., Beranger, A., Prud'homme, J.F., Baulac, M., Brice, A., Bruzzone, R., and LeGuern, E. (2001). First genetic evidence of $GABA_A$ receptor dysfunction in epilepsy: a mutation in the γ2-subunit gene. Nat. Genet. *28*, 46–48.

Bennett, P.B., Yazawa, K., Makita, N., and George, A.L., Jr. (1995). Molecular mechanism for an inherited cardiac arrhythmia. Nature *376*, 683–685.

Berkovic, S.F. (2001). Epilepsies. In Channelopathies of the Nervous System, M.R. Rose and R.C. Griggs, eds. (Oxford: Butterworth Heinemann), pp. 239–249.

Browne, T.R., and Holmes, G.L. (2001). Epilepsy. N. Engl. J. Med. *344*, 1145–1151.

Cannon, S.C. (2000). Spectrum of sodium channel disturbances in the nondystrophic myotonias and periodic paralyses. Kidney Int. *57*, 772–779.

Cannon, S.C., Brown, R.H., Jr., and Corey, D.P. (1993). Theoretical reconstruction of myotonia and paralysis caused by incomplete inactivation of sodium channels. Biophys. J. *65*, 270–288.

Catterall, W.A. (1992). Cellular and molecular biology of voltage-gated sodium channels. Physiol. Rev. *72*, S15–S48.

Catterall, W.A. (1999). Molecular properties of brain sodium channels: an important target for anticonvulsant drugs. Adv. Neurol. *79*, 441–456.

Claes, L., Del Favero, J., Ceulemans, B., Lagae, L., Van Broeckhoven, C., and De Jonghe, P. (2001). De novo mutations in the sodium-channel gene SCN1A cause severe myoclonic epilepsy of infancy. Am. J. Hum. Genet. *68*, 1327–1332.

Dudek, F.E., Yasumura, T., and Rash, J.E. (1998). "Non-synaptic" mechanisms in seizures and epileptogenesis. Cell Biol. Int. *22*, 793–805.

Escayg, A., MacDonald, B.T., Meisler, M.H., Baulac, S., Huberfeld, G., An-Gourfinkel, I., Brice, A., LeGuern, E., Moulard, B., Chaigne, D., et al. (2000). Mutations of SCN1A, encoding a neuronal sodium channel, in two families with GEFS+2. Nat. Genet. *24*, 343–345.

Escayg, A., Heils, A., MacDonald, B.T., Haug, K., Sander, T., and Meisler, M.H. (2001). A novel *SCN1A* mutation associated with generalized epilepsy with febrile seizures plus - and prevalence of variants in patients with epilepsy. Am. J. Hum. Genet. *68*, 866–873.

Goldin, A.L., Barchi, R.L., Caldwell, J.H., Hofmann, F., Howe, J.R., Hunter, J.C., Kallen, R.G., Mandel, G., Meisler, M.H., Netter, Y.B., et al. (2000). Nomenclature of voltage-gated sodium channels. Neuron *28*, 365–368.

Hamill, O.P., Marty, A., Neher, E., Sakmann, B., and Sigworth, F.J. (1981). Improved patch-clamp techniques for high-resolution current recording from cells and cell-free membrane patches. Pflügers Arch. *391*, 85–100.

Jefferys, J.G. (1995). Nonsynaptic modulation of neuronal activity in the brain: electric currents and extracellular ions. Physiol. Rev. *75*, 689–723.

Krafte, D.S., Goldin, A.L., Auld, V.J., Dunn, R.J., Davidson, N., and Lester, H.A. (1990). Inactivation of cloned Na channels expressed in *Xenopus* oocytes. J. Gen. Physiol. *96*, 689–706.

Macdonald, R.L., and Greenfield, L.J., Jr. (1997). Mechanisms of action of new antiepileptic drugs. Curr. Opin. Neurol. *10*, 121–128.

Matsumoto, H., and Ajmone-Marsan, C. (1964). Cortical cellular phenomena in experimental epilepsy. Exp. Neurol. *9*, 305–326.

McCormick, D.A., and Contreras, D. (2001). On the cellular and network bases of epileptic seizures. Annu. Rev. Physiol. *63*, 815–846.

Meisler, M.H., Kearney, J., Ottman, R., and Escayg, A. (2001). Identification of epilepsy genes in human and mouse. Annu. Rev. Genet. *35*, 567–588.

Moorman, J.R., Kirsch, G.E., VanDongen, A.M.J., Joho, R.H., and Brown, A.M. (1990). Fast and slow gating of sodium channels encoded by a single mRNA. Neuron *4*, 243–252.

Reckziegel, G., Beck, H., Schramm, J., Elger, C.E., and Urban, B.W. (1998). Electrophysiological characterization of Na^+ currents in acutely isolated human hippocampal dentate granule cells. J. Physiol. (London) *509 Pt 1*, 139–150.

Sah, D.W. (1995). Human fetal central neurons in culture: voltage- and ligand-gated currents. J. Neurophysiol. *74*, 1889–1899.

Scheffer, I.E., and Berkovic, S.F. (1997). Generalized epilepsy with febrile seizures plus. A genetic disorder with heterogeneous clinical phenotypes. Brain *120 Pt 3*, 479–490.

Segal, M.M. (1991). Epileptiform activity in microcultures containing one excitatory hippocampal neuron. J. Neurophysiol. *65*, 761–770.

Segal, M.M. (1994). Endogenous bursts underlie seizurelike activity in solitary excitatory hippocampal neurons in microcultures. J. Neurophysiol. *72*, 1874–1884.

Segal, M.M. (2002). Sodium channels and epilepsy electrophysiology. Novartis Found. Symp. *241*, 173–180.

Shin, C., and McNamara, J.O. (1994). Mechanism of epilepsy. Annu. Rev. Med. *45*, 379–389.

Singh, R., Scheffer, I.E., Crossland, K., and Berkovic, S.F. (1999). Generalized epilepsy with febrile seizures plus: a common childhood- onset genetic epilepsy syndrome. Ann. Neurol. *45*, 75–81.

Spampanato, J., Escayg, A., Meisler, M.H., and Goldin, A.L. (2001). Functional effects of two voltage-gated sodium channel mutations that cause generalized epilepsy with febrile seizures plus type 2. J. Neurosci. *21*, 7481–7490.

Sugawara, T., Tsurubuchi, Y., Agarwala, K.L., Ito, M., Fukuma, G., Mazaki-Miyazaki, E., Nagafuji, H., Noda, M., Imoto, K., Wada, K., et al. (2001a). A missense mutation of the Na^+ channel α_{II} subunit gene $Na_v1.2$ in a patient with febrile and afebrile seizures causes channel dysfunction. Proc. Natl. Acad. Sci. USA *98*, 6384–6389.

Sugawara, T., Mazaki-Miyazaki, E., Ito, M., Nagafuji, H., Fukuma, G., Mitsudome, A., Wada, K., Kaneko, S., Hirose, S., and Yamakawa, K. (2001b). $Na_v1.1$ mutations cause febrile seizures associated with afebrile partial seizures. Neurology *57*, 703–705.

Wallace, R.H., Wang, D.W., Singh, R., Scheffer, I.E., George, A.L., Jr., Phillips, H.A., Saar, K., Reis, A., Johnson, E.W., Sutherland, G.R.,

et al. (1998). Febrile seizures and generalized epilepsy associated with a mutation in the Na^+-channel β1 subunit gene *SCN1B*. Nat. Genet. *19*, 366–370.

Wallace, R.H., Marini, C., Petrou, S., Harkin, L.A., Bowser, D.N., Panchal, R.G., Williams, D.A., Sutherland, G.R., Mulley, J.C., Scheffer, I.E., and Berkovic, S.F. (2001a). Mutant $GABA_A$ receptor γ2-subunit in childhood absence epilepsy and febrile seizures. Nat. Genet. *28*, 49–52.

Wallace, R.H., Scheffer, I.E., Barnett, S., Richards, M., Dibbens, L., Desai, R.R., Lerman-Sagie, T., Lev, D., Mazarib, A., Brand, N., et al. (2001b). Neuronal sodium-channel α1-subunit mutations in generalized epilepsy with febrile seizures plus. Am. J. Hum. Genet. *68*, 859–865.

Zhou, J., Potts, J.F., Trimmer, J.S., Agnew, W.S., and Sigworth, F.J. (1991). Multiple gating modes and the effect of modulating factors on the μI sodium channel. Neuron *7*, 775–785.